

This is a repository copy of *Prediction of alkaline earth elements in bone remains by near infrared spectroscopy*.

White Rose Research Online URL for this paper:

<https://eprints.whiterose.ac.uk/110415/>

Version: Accepted Version

Article:

Cascant, Mari Merce, Rubio, S, Gallelo, Gianni et al. (3 more authors) (2017) Prediction of alkaline earth elements in bone remains by near infrared spectroscopy. *Talanta*. pp. 428-434. ISSN 0039-9140

Reuse

This article is distributed under the terms of the Creative Commons Attribution-NonCommercial-NoDerivs (CC BY-NC-ND) licence. This licence only allows you to download this work and share it with others as long as you credit the authors, but you can't change the article in any way or use it commercially. More information and the full terms of the licence here: <https://creativecommons.org/licenses/>

Takedown

If you consider content in White Rose Research Online to be in breach of UK law, please notify us by emailing eprints@whiterose.ac.uk including the URL of the record and the reason for the withdrawal request.

1 **PREDICTION OF ALKALINE EARTH ELEMENTS IN BONE REMAINS BY NEAR INFRARED**
2 **SPECTROSCOPY**

3 Mari Merce Cascant, Sonia Rubio, Gianni Gallelo*, Agustín Pastor, Salvador Garrigues and
4 Miguel de la Guardia.

5 Department of Analytical Chemistry, University of Valencia,
6 50 Dr. Moliner Street, research building
7 46100 Burjassot, Valencia, Spain.

8 * Corresponding author

9
10 **Abstract**

11 An innovative methodological approach has been developed for the prediction of the
12 mineral element composition of bone remains. It is based on the use of Fourier Transform
13 Near Infrared (FT-NIR) diffuse reflectance measurements. The method permits a fast,
14 cheap and green analytical way, to understand post-mortem degradation of bones caused
15 by the environment conditions on different skeletal parts and to select the best preserved
16 bone samples. Samples, from the Late Roman Necropolis of Virgen de la Misericordia
17 street and En Gil street located in Valencia (Spain), were employed to test the proposed
18 approach being determined calcium, magnesium and strontium in bone remains and
19 sediments. Coefficients of determination obtained between predicted values and
20 reference ones for Ca, Mg and Sr were 90.4, 97.3 and 97.4, with residual predictive
21 deviation of 3.2, 5.3 and 2.3, respectively, and relative root mean square error of
22 prediction between 10 and 37%. Results obtained evidenced that NIR spectra combined
23 with statistical analysis can help to predict bone mineral profiles suitable to evaluate bone
24 diagenesis.

Keywords: NIR, multivariate statistics, alkaline earth elements, buried bones, diagenesis, soil.

1. Introduction

Bone is composed of 50 to 70% mineral, 20 to 40% organic matrix, mainly collagen, 5 to 10% water, and less than 3% lipids. The mineral content of bone is mostly hydroxylapatite $[\text{Ca}_{10}(\text{PO}_4)_6(\text{OH})_2]$, with small amounts of carbonate, magnesium, and acid phosphate, with missing hydroxyl groups that are normally present [1]. Under physiologic conditions, hydroxylapatite is the only stable mineral in bones and is composed of 38% of calcium and 18% of phosphorous, with trace of sodium (0,6%), magnesium and small amount of other elements [2]. The number of ionic substitutions possible in biological apatite is smaller than in geologic apatites due to the limited number of available elements in the body. Among the substituting ions that are known and/or reported in bone and tooth mineral are F^- , Cl^- , Na^+ , K^+ , Fe^{2+} , Zn^{2+} , Sr^{2+} , Mg^{2+} , citrate, and carbonate [3].

Minerals are ingested from food or involuntary absorbed from the environment. Chemical composition of bones mineral is commonly employed to investigate pathologies, nutrition, injuries and other bioarchaeological and forensic issues.

The mineral composition of bones can be post-mortem modified by post-depositional processes, called as well diagenesis, and since many decades researchers have been intensively studied these natural mechanisms. Some authors have evaluated post-mortem soil contamination in bones [4-9]. Other authors have studied diagenesis and degradation effects on bone matrix [10-13].

48 Calcium, oxygen and hydrogen are major constituents of mineral bones as hydroxylapatite
49 [14]. Strontium is a non-essential trace element that competes to replace calcium[15]and
50 has been linked to food consumption habits [16]. The soil composition and environmental
51 conditions play a crucial role in diagenesis, affecting the element concentration of the
52 buried bones.

53 The general aims of this study has been to develop a low cost, clean and fast strategy to
54 understand how post-mortem degradation in bones caused by the environment could
55 affect different skeletal parts and define an approach to select the best preserved bone
56 samples. Therefore, a method for the determination of mineral elements in bone remains
57 has been developed employing Fourier Transform Near Infrared (FT-NIR) spectroscopy by
58 using chemometric tools as principal component analysis (PCA) and Partial Least Square
59 (PLS). Inductively-Coupled Plasma Optical Emission Spectroscopy (ICP-OES) results have
60 been used as reference data to create prediction models.

61 ICP-OES has been commonly used as an accurate procedure to determine mineral
62 elements in soils and bones [17-21]. ICP-OES technique is very useful for multi-element
63 analysis. However it requires a previous sample digestion and dissolution, involving the
64 use of strong acids and providing non-degradable wastes. A green alternative to the
65 aforementioned technique could be infrared (IR) spectroscopy which provides fast
66 spectral acquisition, a cheap acquisition and maintenance cost and a sustainable method,
67 since it does not use reagents and can be employed directly on solid samples.
68 Combination of IR spectroscopy with chemometric data analysis could offer a significant

tool for the determination of major components of bones and sediments including mineral elements.

Fourier Transform infrared (FT-IR) spectroscopy of bones has been used for various applications as collagen determination, bone crystal size, some carbonates and crystalline structure [22-25], and geochemical taphonomy [26] and as screening tool for diagenetic alteration [27, 28]. On the other hand, only few studies have employed NIR for soils [29] and bones analysis [30] in archaeological contexts.

In the present study, two hundred seventy one samples obtained from at least 78 individuals, have been analyzed. Samples belong to adult and young individuals and are from the Late Roman Necropolis of Virgen de la Misericordia Street [19] and en Gil Street [31], both located in the city of Valencia (Spain). The Late Roman burial rite consisted in inhumation. At this sites, the tombs belong to the period from the I century A.D. until the beginning of the V century A.D.

Bone samples were collected from femur, tibia, humerus, radius and parietal bones, which were classified as cortical bones, and ribs as spongy bones. Furthermore, bone samples from the outer bone layer and soil samples were analyzed. Outer bone layer samples were obtained from the external bone surface directly in contact with the sediments. Principal Component Analysis (PCA) was applied to identify bone samples with a well preserved elemental composition. Therefore for the first time Partial Least Square (PLS) regression models were built to predict the concentration of calcium, magnesium and strontium in skeletal remains by NIR spectra of the mineralized and homogenized solid samples.

2. Materials and methods

2.1. Sample collection

Bone samples were collected from 78 different individuals, sampling around 5 cm of each bone and the weight of the collected sample ranged between 15 and 20 grams depending on the type of bone. Bones as femur, tibia, humerus, radius and parietals, mainly composed by a cortical matrix were classified as “cortical”, and ribs mainly composed by a spongy matrix were grouped as “spongy”. The first 2 mm of bone directly in contact with the sediments was called external part of bones and was obtained employing a bistoury to scrape. All bones were sampled avoiding the osteometric points, and the sampling was carried out using a cutting toll and a micro spoon spatula.

To provide reproducible and comparable results compatible with the sensitivity of the analytical methods employed and so appropriately relate NIR obtained data with the reference method data all samples were previously mineralized in a muffle furnace, (temperature programme employed: I. 30min at 150 °C; II. 1° /min up to 450 °C; III. 24h at 450 °C; IV. 30 °C), and pulverized and homogenized with an agate mortar

A total of 243 samples from Virgen de la Misericordia were analysed. Bone samples were divided in three groups: i) internal part of bones, composed by the internal part of cortical and spongy ones (95 samples), ii) external part of bones, composed by the first external layer of cortical bones and spongy ones (94 samples) and, iii) sediments that were directly

in contact with the bones (54 samples). Additionally following the mentioned classification, 28 samples from En Gil internal part of bones (8 samples), external part of bones (10 samples) and sediments (10 samples) were also analyzed.

2.2. Apparatus and methods

For diffuse reflectance near infrared spectra acquisition, a Fourier transform near infrared spectrometer, model Multipurpose Analyzer (MPA) from Bruker (Bremen, Germany), equipped with an integrating sphere was employed. This instrument is equipped with a NIR source, a quartz beamsplitter and PbS detector. For instrumental and measurement control as well as for data acquisition, Opus 6.5 software from Bruker was used.

References values about the mineral composition of samples were determined by using an Optima 5300 DV ICP-OES Perkin Elmer (Norwalk, CT, USA) equipped with an autosampler AS 93-plus and a cross flow nebuliser. Samples were previously calcinated inside a muffle furnace Biometa Lenton ECF 12145A (Lanera, España) and acid digested using a heating plate Ika C-Mag HS7.

2.3. Reference method

The digestion method was developed modifying the process described by Gallello et al. 2013 and 2014 [19] and consisted in addition to 0.5 g of mineralized sample of 1:1 HCl and HNO₃ (using 37 % HCl and 69 % HNO₃ high purity stock) and digested in a water bath at 100° C. This concentrated solution (A), was diluted 1:250 obtaining solution (B), to

measure Mg and Sr. Solution (C) was obtained to analyze Ca by diluting 1:2000 solution (A). Concentrations of HCl and HNO₃ have been maintained constant in all solutions. A multi-element stock solution containing Ca, Mg and Sr at a concentration of 100 µg ml⁻¹ was employed for the preparation of the calibration standards in 50 ml volumetric flasks. To avoid the obstruction of the nebulizer system samples were filtered employing filter paper (WhatmanTM N.1 of 70mm). Concentrations ranging between 0 and 20 µg ml⁻¹ were used for Ca, Mg and Sr. Standards were obtained from Sharlab S.L. (Barcelona, Spain). The standard error of readings during the analysis ranged from 0 % to 2 % for the major elements considered. Bone ash NIST 1400 and soil GBW07408 were used as standard reference materials for evaluating the accuracy of the analytical method and Re was used as internal standard. Mineral element content of studied samples, determined by reference method, varied between 72 and 421 mg g⁻¹ for calcium, 998 and 10964 µg g⁻¹ for magnesium and, 102 and 2100 µg g⁻¹ for strontium.

2.4. NIR procedure

Pulverized mineralized samples were placed in clear glass vials of 11 mm internal diameter and 25 mm height to directly obtain their NIR spectra by diffuse reflectance in Kubelka–Munk units. Spectra were collected between 14000 and 4000 cm⁻¹ by averaging 50 scans and using an optical resolution of 4 cm⁻¹. A background spectrum was acquired before each series, from the closed integrating sphere using the same instrumental conditions than those employed for samples measurement. Three measurements of each sample were obtained by rotating the sample vial position between replicates in order to ensure a

good reliability. The average of the triplicate spectra of each sample was employed for data exploration and to build the chemometric models.

2.5. Chemometric data treatment

Data treatment was carried out using in-house written functions employing Matlab 8.3.0.532 (R2014a) from Mathworks (Natick, MA, USA) being employed for Principal Analysis Components (PCA) and Partial least squares (PLS) regression model, the PLS Toolbox 7.5.2 from Eigenvector Research Inc. (Wenatchee, WA, USA).

PCA applied to IR spectra was used as data exploration; based on the distance between samples the evaluation of their similarity. PLS models were applied to spectral data to develop prediction models for Ca, Mg and Sr. These calibration models were developed based on the statistically inspired modification of the PLS method (SIMPLS) algorithm [32]. To select the most appropriate sample calibration set, Kennard–Stone (KS) algorithm [33] was used, thus selecting a representative subset to ensure training samples spread evenly throughout the sample space. For building the best PLS models, different spectral regions and spectra pre-treatments were tested as multiplicative scatter correction (MSC), standard normal variation (SNV), a Savitzky-Golay first (FD) and second derivative (SD), and mean center (MC) also combination of them. The performance of PLS-NIR models was evaluated according to the root mean square error of cross validation and prediction (RMSECV and RMSEP) values, the coefficient of determination for prediction (R^2_{pred}), relative root mean square error of prediction (RRMSEP) and residual predictive deviation (RPD), calculated this last parameter as the

ratio between standard deviation (SD) of the prediction set and the RMSEP values [34]. Generally, RPD value greater than 3.0 is considered adequate for analytical purposes with excellent prediction accuracy, between 2.5 and 3.0 implies that the model has a good precision and between 2.0 and 2.5 indicates that the model has an approximate precision. A value for the RPD between 1.5 and 2.0 reveals a possibility to distinguish between high and low values and a RPD 1.5 indicates that the calibration is not usable [35]. The optimum number of latent variables (LV's) was determined by cross-validation using leave one out sample in order to obtain the minimum value of RMSECV.

3. Results and discussion

3.1. FT-NIR spectra

Figure 1 shows, in Kubelka Munk units, the averaged NIR spectra of a) internal part, b) external part of bones and c) sediment samples, considered in this study without any data pre-treatment, in the region between 9000 and 4000 cm^{-1} . These sample spectra present differences in the intensity and position of certain bands, but all show absorption bands around 7200 and 5220 cm^{-1} related to combination vibrations of H–O–H bend and O–H stretch of water. The main difference which presents internal bones is the weak vibration which appear near 4655 cm^{-1} (without a clear assignment) and the absorption near 6977 cm^{-1} assigned to the first overtone of the stretching vibrations of OH group in hydroxyapatite [36], that is higher than in external part of bones. In the case of the sediment samples, the aforementioned band is absent. Additionally, at 5278 cm^{-1} , internal part of bone and external part of bone in minor intensity, present an absorption band

related to apatite [30]. On the other hand, in sediment samples it is present a band at 7070 cm^{-1} related to the first overtone of the O–H stretch vibration in metal–O–H [37]. Moreover, vibrations bands near of 4530 cm^{-1} are due to clay minerals, like smectite and illite, and the band at 4265 cm^{-1} is associated with the contribution of calcite [37], which decreases in intensity in external bone. In the case of internal part of bone samples, the band located at 4265 cm^{-1} not appears and the band at 4530 cm^{-1} is less intense than in external part of bones. So that, in external part of bones appear typical bands of sediment samples related with metal-OH (7070 cm^{-1}), calcite (4265 cm^{-1}) and clay minerals (4530 cm^{-1}), and lower bands of hydroxyapatite (6977 cm^{-1}) and apatite (5278 cm^{-1}). Degradation of hydroxyapatite in external part of bones is a great indicator of diagenetic process. Sediments around bones are crucial role to conservation of them, and sediments analysis should be carried out in order to assess their contribution to the modification of the bone chemical composition.

3.2. Data Exploration by PCA

Before building the calibration models, PCA was used for exploratory data analysis to study the spectral differences between considered samples. Figure 2 presents the scores plot for first and the second principal components obtained from PCA for Misericordia and En Gil Necropolis, after a) FD and MC and b) MSC, FD and MC pre-treatment, being selected the region from $9014\text{ to }4000\text{ cm}^{-1}$. In Figure 2a, the two first principal components after spectra pretreatment by using FD and MC represent 86.07% of the

explained variance, being 76.93 and 9.14% for PC1 and PC2, respectively. In the scores plot, there is not a clear-cut grouping of samples, but it can be appreciated that sediment samples spectra are clearly different from those of internal part of bone samples and that, external part of bone samples are located between sediment and internal part of bone ones in the direction of PC1. In Figure 2b, it can be seen that the scores plot for first and the second principal components after MSC, FD and MC pretreatment, represent 85.72% of the explained variance (PC1 corresponds to 80.49% and PC2 corresponds to 5.23% of the variance). It can be seen that internal part of bone samples are located towards the right of the PC1 and sediment samples are dispersed in the left. External part of bone samples are situated between these two groups in the direction of PC1. Moreover, PCA indicates that samples derived from En Gil are similar to Misericordia samples, and because of that samples from Misericordia can be used as calibration set to predict alkaline earth elements in En Gil samples.

The aforementioned PCAs were built using differentiated internal and external parts of bones in both, spongy and cortical remains. Figure 2c presents the scores plot after FD and MC and Figure 2d after MSC, FD and MC pretreatment. No differences were detected between internal parts of cortical and spongy bones. However if we look at the external part of bones, spongy group is located near to sediment samples, and external part of cortical bones are located close to internal part of bones because spongy tissues are more susceptible to diagenesis than cortical [38] due to the fragility and porosity of their structure. Wavenumbers responsible for the distinction of the samples in PCA can be

identified in the corresponding loading plots (Figure 2e and 2f) with a clear identification of bands around 7000 cm^{-1} and between 5500 and 4000 cm^{-1} .

So, it can be concluded that PCA analysis using NIR spectra data provides a fast and green tool to identify changes caused by the environment in bone samples. These results indicate that external part of bones suffer an increased degradation produced by diagenetic factors than internal part of bones, especially in the case of spongy bones external part due to their high porosity. Consequently, conclusions about identification of biogenetic signals using major element ratios could change depending of the bone class evaluated. To avoid mistakes, the use of PCA analysis, as exploratory method, permits a prior selection of samples, not affected by diagenetic processes, to be used in different bioarchaeological and forensic studies involved in bone analyses. Additionally, PCA is a good indicator to test if the calibration set contains the validation samples in order to be used in PLS models without errors due to extrapolation of data.

3.3. PLS-NIR models

To build PLS models, Misericordia samples were divided into a calibration and a validation subset with 183 and 60 objects, respectively, using K-S algorithm for the training set selection, composed by 62 external part of bones, 70 internal part of bones and 51 sediment samples.

The main characteristics of calibration and validation sets selected for the three elements determination by PLS-NIR are indicated in Table 1. Several regions and different pre-

processing strategies were assayed to build the best models and to evaluate their prediction capability. For all elements, regions selected were those between 9014 and 4000 cm^{-1} . To build PLS-NIR models using the selected spectral range, 3, 4 and 4 LVs were employed for Ca, Mg and Sr, respectively, in order to minimize the RMSECV, explaining 89.1 %, 90.8 % and 88.5 % of the total variance of the X data block and 92.4%, 95.0% and 90.4% of the Y data block, respectively. For Ca and Mg, FD with a window of 11 points and a second order polynomial, and MC treatment were adopted as signal pre-processing. For strontium, MSC, FD and MC were chosen. Additionally, concentration data were mean centered as well in all cases. Outliers can be identified by Q residual versus the Hotelling T^2 values, being removed 2 samples from the calibration set of Ca, Mg and Sr and 2 samples from the validation set of Ca and Sr and only one sample of Mg, prior to do the calculations and validation of the final PLS models for those elements. Figure 3a shows the regression between PLS-NIR predicted values for Ca, Mg and Sr and those obtained by the reference ICP-OES method. It can be seen that calibration and validation sample points were closely distributed near the optimum regression line between predicted and measured values for the three elements, obtaining high coefficients of determination for calibration (R^2_{cal}), cross validation (R^2_{CV}) and prediction (R^2_{pred}) in all elements. The prediction capability of PLS-NIR models were good for all elements, obtaining RRMSEP values of 10%, 15% and 19% for calcium, magnesium and strontium, respectively. The most important calibration and validation parameters of the developed PLS-NIR models are summarized in Table 2.

It can be seen that samples of internal part of bones contain higher calcium ($368 \pm 24 \text{ mg g}^{-1}$) and strontium ($1306 \pm 235 \text{ } \mu\text{g g}^{-1}$) levels and lower magnesium content ($1393 \pm 175 \text{ } \mu\text{g g}^{-1}$) than external parts (with $261 \pm 47 \text{ mg g}^{-1}$ of Ca, $844 \pm 203 \text{ } \mu\text{g g}^{-1}$ of Sr and $5599 \pm 1684 \text{ } \mu\text{g g}^{-1}$ of Mg) and sediment samples (with $133 \pm 17 \text{ mg g}^{-1}$ of Ca, $239 \pm 60 \text{ } \mu\text{g g}^{-1}$ of Sr and $8165 \pm 858 \text{ } \mu\text{g g}^{-1}$ of Mg). As aforementioned, in physiologic conditions, hydroxylapatite is composed of 38 % Ca, with traces of Mg and small amounts of other elements like Sr, indicating that internal part of bones are intact looking at Ca values that are around the 38%. Mg enrichment in external part of bones indicates that this element is probably incorporated into the bones from sediments during diagenesis process.

External part of bones, especially in the case of spongy bone remains are more sensitive to diagenetic processes caused by the environment indicating that degradation not affects in the same extent different skeletal parts. Due to the fact that spongy bones have higher porosity and thinner cortex than cortical bones, the first type is less resistant to diagenetic factors suffering chemical changes.

Results obtained by PLS-NIR models indicated that NIR spectroscopy has a good potential to predict alkaline earth elements content in bone remains. As mentioned this method has many advantages over the conventional employed analytical techniques because it is quick, inexpensive, non-destructive for pulverized samples and does not require the use of chemical reagents nor solvents.

3.4. PLS-NIR prediction capability

To evaluate the PLS-NIR prediction capability of models built to predict Ca, Mg and Sr concentrations in bones and sediments, an independent validation set, not employed during the calibration step, was used. For this propose external part, internal part of bones and sediment samples of En Gil Necropolis were used as external set. The mean, concentration range and standard deviation for the concentration of analysed elements employed for prediction set are summarized in Table 1. Predicted values of the analytes versus those obtained by the reference methods are shown in Figure 3b and the most important calibration and prediction parameters of the developed NIR-PLS models are summarized in Table 2. Acceptable RRMSEP values were obtained for calcium and magnesium with 15% and 11%, respectively, and for strontium a value of 37% was obtained, with correlation coefficients of 90.4, 97.4 and 97.4, and RPD values of 3.2, 5.33 and 2.3, respectively. These results demonstrate a good predictive capability of the PLS-NIR models developed to evaluate alkaline earth elements in bones and sediment samples.

Furthermore it must be indicated the PLS models were made from bone samples of different origin, and date of those of the training set, confirming the feasibility of our innovative methodological proposal for the evaluation of alkaline earth elements in archaeological remains.

The obtained results indicate a good predictive capability for Mg in samples that not belong to the same population while Ca were predicted with relative errors of 15% and Sr

37%, respectively, being thus limited as a screening tool. Especially for Sr the high relative error of 37% is probably due to the lower levels of this element found in some samples not compatible with the sensitivity of NIR.

4. Conclusions

Fourier Transform Near Infrared (FT-NIR) provides a fast, cheap and green analytical method for the prediction of the content of calcium, magnesium and strontium in buried bone and sediment samples, and it could be very useful to understand post-mortem changes of bones caused by the environment which can affects different skeletal parts and for selecting bone samples with well preserved biogenetic signals. PCA has shown that the alkaline earth element profile of bone and soil samples, as expected, is clearly different. Furthermore the external surface of spongy bones is more similar to the soils than to the surface of cortical bones. This confirm that the outer bone layer of spongy bones is more altered than the cortical surface and the presence of Ca, Mg and Sr is similar to that of soil samples of the studied sites. Therefore it can be concluded that environmental factors have a main impact on spongy tissues, which are more susceptible to diagenetic processes, than on the cortical bones. It is indicated in the NIR spectra by the loss of apatite band (the main bone compound) and the presence of clay bands especially on spongy bone surface.

A milestone in the study of bone remains is settled in this work by the development of PLS-NIR models, indicating that FT-NIR spectroscopy can be employed to predict Ca, Mg

and Sr contents in bones remains and soils samples. Ca and Sr contents were found to be higher in the internal part of bone samples, opposite to Mg contents that were higher in the external bone surface and soils, and lower in internal part of bones. Our developed methodological approach combines NIR spectroscopy and statistical analysis and this allowed us to predict bone alkaline earth mineral composition opening a new perspective for the identification of better preserved samples in bioarchaeological studies and forensic science investigations.

Regarding the limitations of the study it must be noticed that it was based only on the mineral part of skeletal remains which were treated thermally and pulverized before measurements thus losing information from the organic part of bones and soils. Additionally, the lack of sensitivity of NIR spectroscopy seriously affected the capability of these measurements to be employed for trace element determination and just important elements present as major components of bones, like Ca, Mg and Sr could be determined.

Acknowledgements

Authors acknowledge the financial support of Generalitat Valenciana (Project **PROMETEO II/2014/077**) and **Ministerio de Economía y Competitividad-Feder** (Projects **CTQ 2014-52841-P** and **CTQ 2012-38635**). M.C acknowledges the FPI grant (**BES-2012-055404**) provided by the **Ministerio de Economía y Competitividad** of the Spanish government.

The authors would like to thanks all the students of Chemistry and Archaeology which have contributed to the realization of this study.

376

377 **References**

- 378 [1] B. Clarke, Normal bone anatomy and physiology, *Clin. J. Am. Soc. Nephrol.* 3 (2008) Suppl 3,
379 S131–139.
- 380 [2] J. Burton, Bone chemistry and trace element analysis. in M.A. Katzenberg, S.R. Saunders
381 (Eds.) *Biological anthropology of the human skeleton*. 2nd ed. John Wiley & Sons, Inc.,
382 Hoboken, NJ (2008) 443–460.
- 383 [3] B. Wopenka and J. D. Pasteris, A mineralogical perspective on the apatite in bone, *Mater. Sci.*
384 *Eng. C*, 25 (2005) 131–143.
- 385 [4] R. E. M. Hedges and A. R. Millard, Bones and Groundwater: Towards the Modelling of
386 Diagenetic Processes, *J. Archaeol. Sci.*, 22 (1995) 155–164.
- 387 [5] R. E. M. Hedges, Bone diagenesis: an overview of processes, *Archaeometry*, 44 (2002) 319–
388 328.
- 389 [6] W. Querido, A. L. Rossi, and M. Farina, The effects of strontium on bone mineral: A review on
390 current knowledge and microanalytical approaches, *Micron*, 80 (2016), 122–134.
- 391 [7] J. B. Lambert, L. Xue, and J. E. Buikstra, Inorganic analysis of excavated human bone after
392 surface removal, *J. Archaeol. Sci.*, 18 (1991) 363–383.
- 393 [8] F. Donald Pate and J. T. Hutton, The Use of Soil Chemistry Data to Address Post-mortem
394 Diagenesis in Bone Mineral, *J. Archaeol. Sci.*, 15 (1988) 729–39.
- 395 [9] J. Zapata, C. Pérez-Sirvent, M. Martínez-Sánchez, and P. Tovar, Diagenesis, not biogenesis:
396 Two late Roman skeletal examples, *Sci. Total Environ.*, 369 (2006) 357–368.
- 397 [10] I. Reiche, L. Favre-Quattropani, Calligaro, T. J. S., H. Bocherens, L. Charlet, M. Menu, Trace
398 element composition of Archaeological Bones and postmortem alteration in the burial
399 environment. *Nuclear Instruments and Methods. Physics Research B* 150 (1999) 656-662.
- 400 [11] I. Reiche, L. Favre-Quattropani, C. Vignaud, H. Bocherens, L. Charlet, M. Menu, A multi-
401 analytical study of bone diagenesis: the Neolithic site of Bercy (Paris, France). *Meas. Sci.*
402 *Technol.* 14 (2003) 1608-1619.
- 403 [12] T.H. Schmidt-Schultz, M. Schultz, Intact protein molecules in archaeological bones – Bone
404 matrix as a treasure chest of ancient diseases and living conditions. *American Journal of*
405 *Physical Anthropology*. Annual Meeting Issue 1999, Wiley-Liss, p. 230.
- 406 [13] T. A. Surovell and M. C. Stiner, Standardizing Infra-red Measures of Bone Mineral
407 Crystallinity: an Experimental Approach, *J. Archaeol. Sci.*, 28(2001) 633–642.
- 408 [14] F. Ignac, G. Gopinath, and V. der W. Hans, *Radionuclide and Hybrid Bone Imaging*. Springer
409 Heidelberg New York Dordrecht London, 2012.

- 410 [15] M. L. Carvalho and A. F. Marques, Diagenesis evaluation in Middle Ages human bones using
411 EDXRF, X-Ray Spectrom., 37 (2008) 32–36.
- 412 [16] D. Guimarães, A. A. Dias, M. Carvalho, M. L. Carvalho, J. P. Santos, F. R. Henriques, F. Curate,
413 and S. Pessanha, Quantitative determinations and imaging in different structures of buried
414 human bones from the XVIII-XIXth centuries by energy dispersive X-ray fluorescence –
415 Postmortem evaluation, Talanta, 155 (2016) 107–115.
- 416 [17] G. Gallelo, J. Kuligowski, A. Pastor, A. Diez, and J. Bernabeu, Biological mineral content in
417 Iberian skeletal remains for control of diagenetic factors employing multivariate statistics, J.
418 Archaeol. Sci., 40(2013) 2477–2484.
- 419 [18] A.-F. Maurer, M. Gerard, A. Person, I. Barrientos, C. R. del, V. Darras, C. Durlet, V. Zeitoun, M.
420 Renard, and B. Faugère, Intra-skeletal variability in trace elemental content of Precolumbian
421 Chupicuaro human bones: The record of post-mortem alteration and a tool for palaeodietary
422 reconstruction, J. Archaeol. Sci., 38 (2011) 1784–1797.
- 423 [19] G. Gallelo, J. Kuligowski, A. Pastor, A. Diez, and J. Bernabeu, Chemical element levels as a
424 methodological tool in forensic science, J Forensic Res, 6 (2014) 1000264.
- 425 [20] A.-F. Maurer, A. Person, T. Tütken, S. Amblard-Pison, and L. Ségalen, Bone diagenesis in arid
426 environments: An intra-skeletal approach, Palaeogeogr. Palaeoclimatol. Palaeoecol., 416
427 (2014) 17–29.
- 428 [21] S. Dal, L. Maritan, D. Usai, I. Angelini, and G. Artioli, Bone diagenesis at the micro-scale: Bone
429 alteration patterns during multiple burial phases at Al Khiday (Khartoum, Sudan) between
430 the Early Holocene and the II century AD, Palaeogeogr. Palaeoclimatol. Palaeoecol.,
431 416(2014) 30–42.
- 432 [22] S. W. Keenan, A. S. Engel, A. Roy, and G. Lisa Bovenkamp-Langlois, Evaluating the
433 consequences of diagenesis and fossilization on bioapatite lattice structure and composition,
434 Chem. Geol., 413 (2015) 18–27.
- 435 [23] C. N. Trueman, K. Privat, and J. Field, Why do crystallinity values fail to predict the extent of
436 diagenetic alteration of bone mineral?, Palaeogeogr. Palaeoclimatol. Palaeoecol., 266
437 (2008)160–167.
- 438 [24] T. J. U. Thompson, M. Islam, K. Piduru, and A. Marcel, An investigation into the internal and
439 external variables acting on crystallinity index using Fourier Transform Infrared Spectroscopy
440 on unaltered and burned bone, Palaeogeogr. Palaeoclimatol. Palaeoecol., 299(2011) 168–
441 174.
- 442 [25] T. J. U. Thompson, M. Islam, and M. Bonniere, A new statistical approach for determining the
443 crystallinity of heat-altered bone mineral from FTIR spectra, J. Archaeol. Sci., 40 (2013) 416–
444 422.
- 445 [26] G. Iliopoulos, N. Galanidou, S. A. Pergantis, V. Vamvakaki, and N. Chaniotakis, Identifying the
446 geochemical taphonomy of the osteological material from Katsambas rockshelter, J.
447 Archaeol. Sci., 37 (2010) 116–123.

- [27] L. E. Wright and H. P. Schwarcz, Infrared and Isotopic Evidence for Diagenesis of Bone Apatite at Dos Pilas, Guatemala: Palaeodietary Implications, *J. Archaeol. Sci.*, 23 (1996) 933–944.
- [28] D. Alfano, A. R. Albunia, O. Motta, and A. Proto, Detection of diagenetic alterations by Spectroscopic Analysis on Archaeological Bones from the Necropolis of Poseidonia (Paestum): A case study, *J. Cult. Herit.*, 10 (2009) 509–513.
- [29] J. Linderholm and P. Geladi, Classification of archaeological soil and sediment samples using near infrared techniques, *NIR News*, 23 (2012) 6.
- [30] D. Thomas, C. McGoverin, A. Chinsamy, and M. Manley, Near infrared analysis of fossil bone from the Western Cape of South Africa, *J. Infrared Spectrosc.*, 19(2011) 151.
- [31] G. Gallelo, S. Silvia, J. Kuligowski, B. Fulvio, M. Francesco, and P. Agustín, Variación química intraesquelética relacionada con la diagénesis en los restos óseos de c/ en Gil (Valencia), *SAGVNTVM*, 47 (2015) 175–186.
- [32] S. de Jong, SIMPLS: An alternative approach to partial least squares regression, *Chemom. Intell. Lab. Syst.*, 3 (1993) 251–263.
- [33] R. W. Kennard and L. A. Stone, Computer Aided Design of Experiments, *Technometrics*, 11 (1969) 137–148.
- [34] P.C. Williams, D. Sobering, How do we do it: A brief summary of the methods we use in developing near infrared calibrations, A.M.C. Daves, P.C. Williams (Eds.), *Near infrared spectroscopy: The future waves*, NIR Publications, Chichester, UK (1995) 185–188.
- [35] W. Saeys, A. M. Mouazen, and H. Ramon, Potential for Onsite and Online Analysis of Pig Manure using Visible and Near Infrared Reflectance Spectroscopy, *Biosyst. Eng.*, 91(2005) 393–402.
- [36] Y. Ning, J. Li, W. Cai, and X. Shao, Simultaneous determination of heavy metal ions in water using near-infrared spectroscopy with preconcentration by nano-hydroxyapatite, *Spectrochim. Acta. A. Mol. Biomol. Spectrosc.*, 96 (2012) 289–294.
- [37] V. Aranda, A. Domínguez-Vidal, F. Comino, J. Calero, and M. J. Ayora-Cañada, Agro-environmental characterization of semi-arid Mediterranean soils using NIR reflection and mid-IR-attenuated total reflection spectroscopies, *Vib. Spectrosc.*, 74 (2014) 88–97.
- [38] J.B. Lambert, S.M. Vlasak, A.C. Thometz, J.E. Buikstra, A comparative study of the chemical analysis of ribs and femurs in Woodland population, *American Journal of Physical Anthropology* 59 (1982) 289–294.

Graphical Abstract

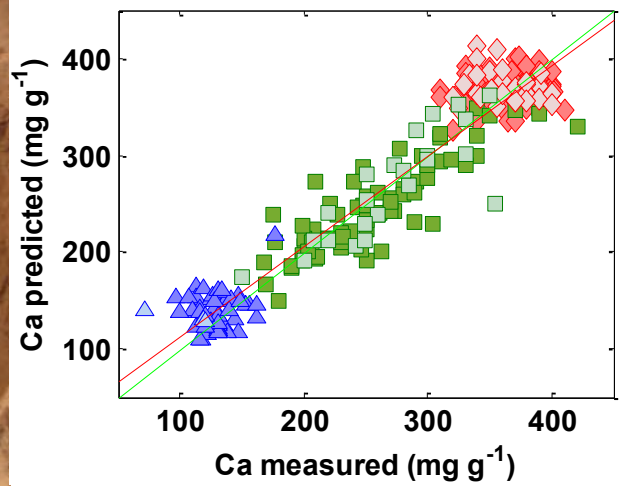
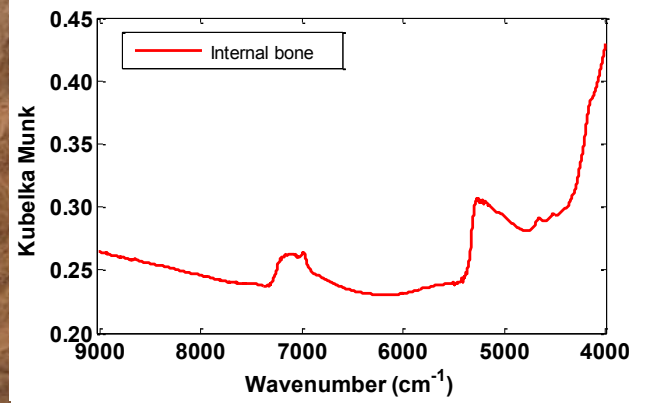


Table 1. Concentration ranges of determined mineral elements in calibration, validation and prediction data sets

Analyte	Set	Samples	Range	Mean value	SD
Calcium (mg g^{-1})	Calibration	181	96 - 421	260	100
Magnesium ($\mu\text{g g}^{-1}$)		181	1050 - 10500	4967	3091
Strontium ($\mu\text{g g}^{-1}$)		181	153 - 2100	823	486
Calcium (mg g^{-1})	Validation	58	72 - 400	312	76
Magnesium ($\mu\text{g g}^{-1}$)		59	1070 - 8500	3226	2545
Strontium ($\mu\text{g g}^{-1}$)		58	124 - 2010	1058	405
Calcium (mg g^{-1})	Prediction	26	112 - 421	233	114
Magnesium ($\mu\text{g g}^{-1}$)		26	998 - 10964	6723	3864
Strontium ($\mu\text{g g}^{-1}$)		26	102 - 1350	518	442

SD: Standard deviation

Table 2. Description of the best PLS-NIR models employed for the determination of Ca, Mg and Sr and their main figures of merit.

Element	Pre-process	LV	Misericordia samples								en Gil samples						
			RMSEC	R ² Cal	RMSECV	R ² CV	RMSEP	R ² Pred	RRMSEP (%)	RPD	RMSEP	R ² Pred	Slope	Intercept	Bias	RRMSEP (%)	RPD
Calcium (mg g ⁻¹)	FD, MC	3	27.5	92.4	29.0	91.6	31.7	83.4	10.2	2.4	35.6	90.4	0.8299	41.4	1.7	15.3	3.2
Magnesium (µg g ⁻¹)	FD, MC	4	686.3	95.0	750.2	94.1	496.6	96.3	15.4	5.1	723.7	97.3	0.9504	246.2	-81.3	10.8	5.3
Strontium (µg g ⁻¹)	MSC, FD, MC	4	150.1	90.4	169.8	87.7	198.9	76.2	18.8	2.0	198.9	97.4	0.9041	78.9	155.0	37.3	2.3

LV: number of latent variables
RMSEC: Root mean square error of calibration; RMSECV: Root mean square error of cross validation; RMSEP: Root mean square error of prediction; RRMSEP: Relative root mean square error of prediction; R² Cal: coefficient of determination of calibration; R² CV: coefficient of determination of cross validation; R² Pred: coefficient of determination of prediction.

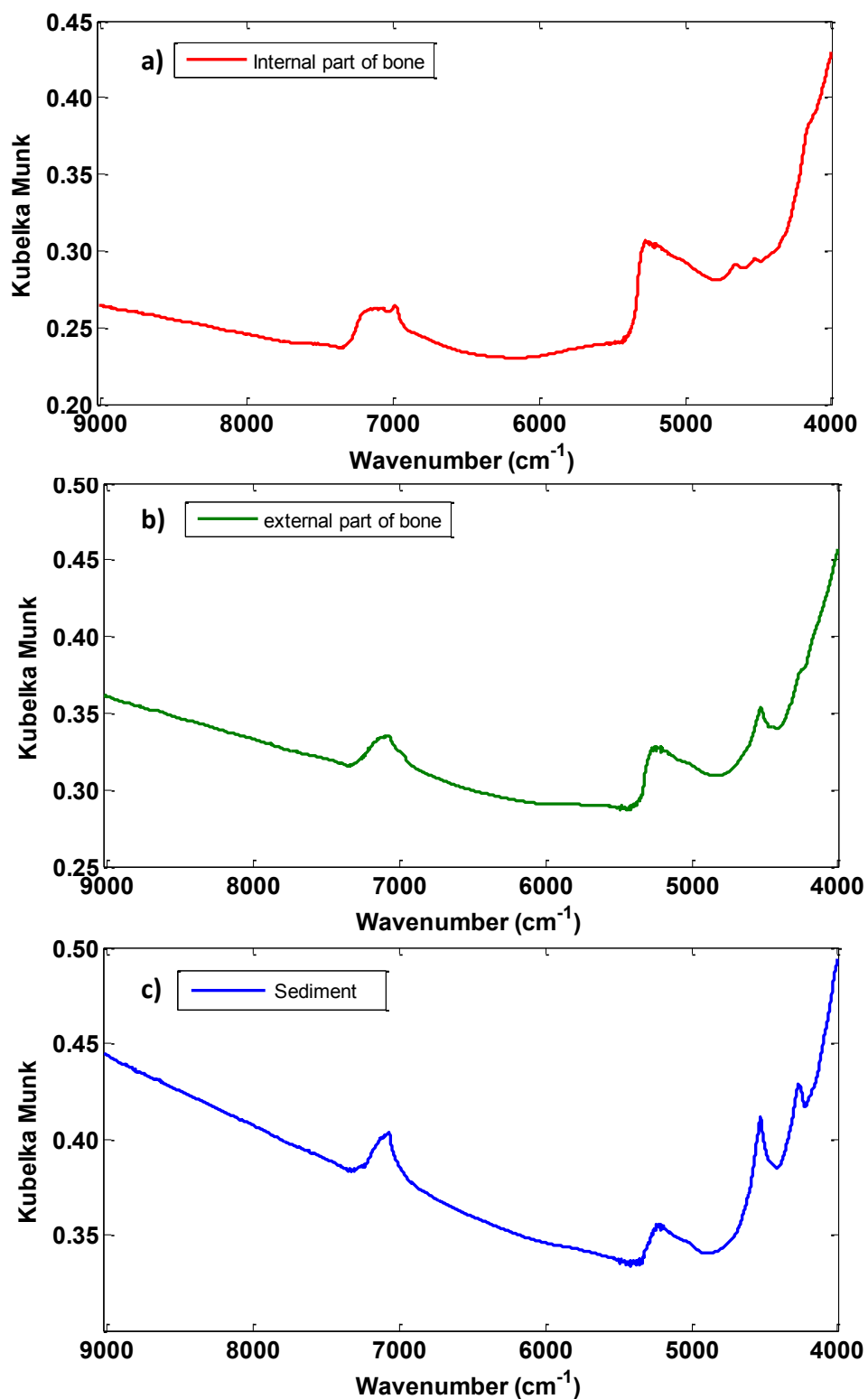


Figure 1. Averaged NIR spectra of mineralized bone and sediment samples comparing **a)** internal part, **b)** external part, and **c)** sediment samples. Note: Spectra were in Kubelka Munk units in the region between 9000 and 4000 cm^{-1} .

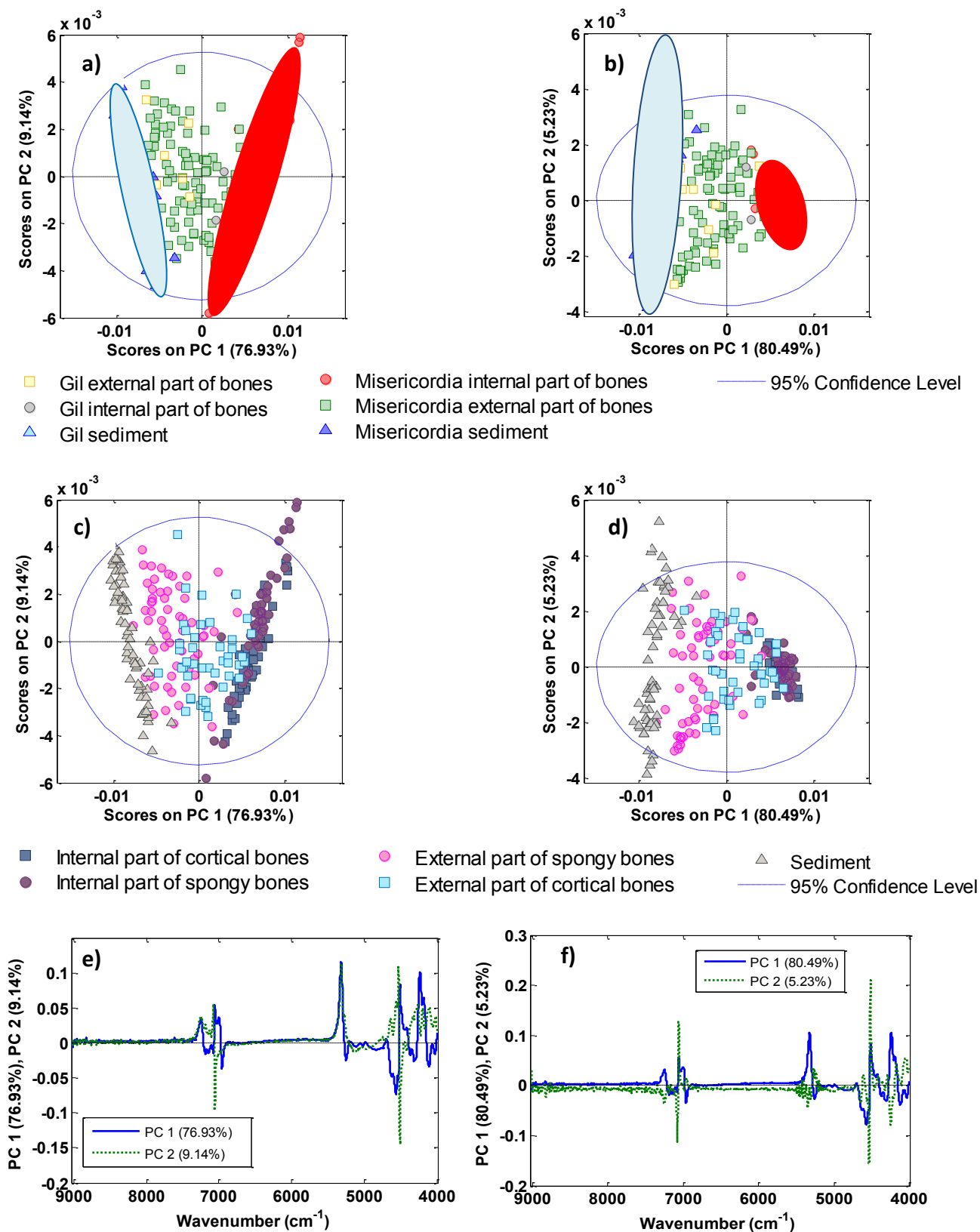


Figure 2. PLS scores and loadings graphs obtained after different spectra treatments. Score plots according Misericordia and En Gil Necropolis sample classification after: **a)** FD and MC, and **b)** MSC, FD and MC pretreatment. Score plots on considering the bone parts after: **c)** FD and MC, and **d)** MSC, FD and MC pretreatment. Loadings of PC1 and PC2 after: **e)** FD and MC, **f)** MSC, FD and MC pretreatment.

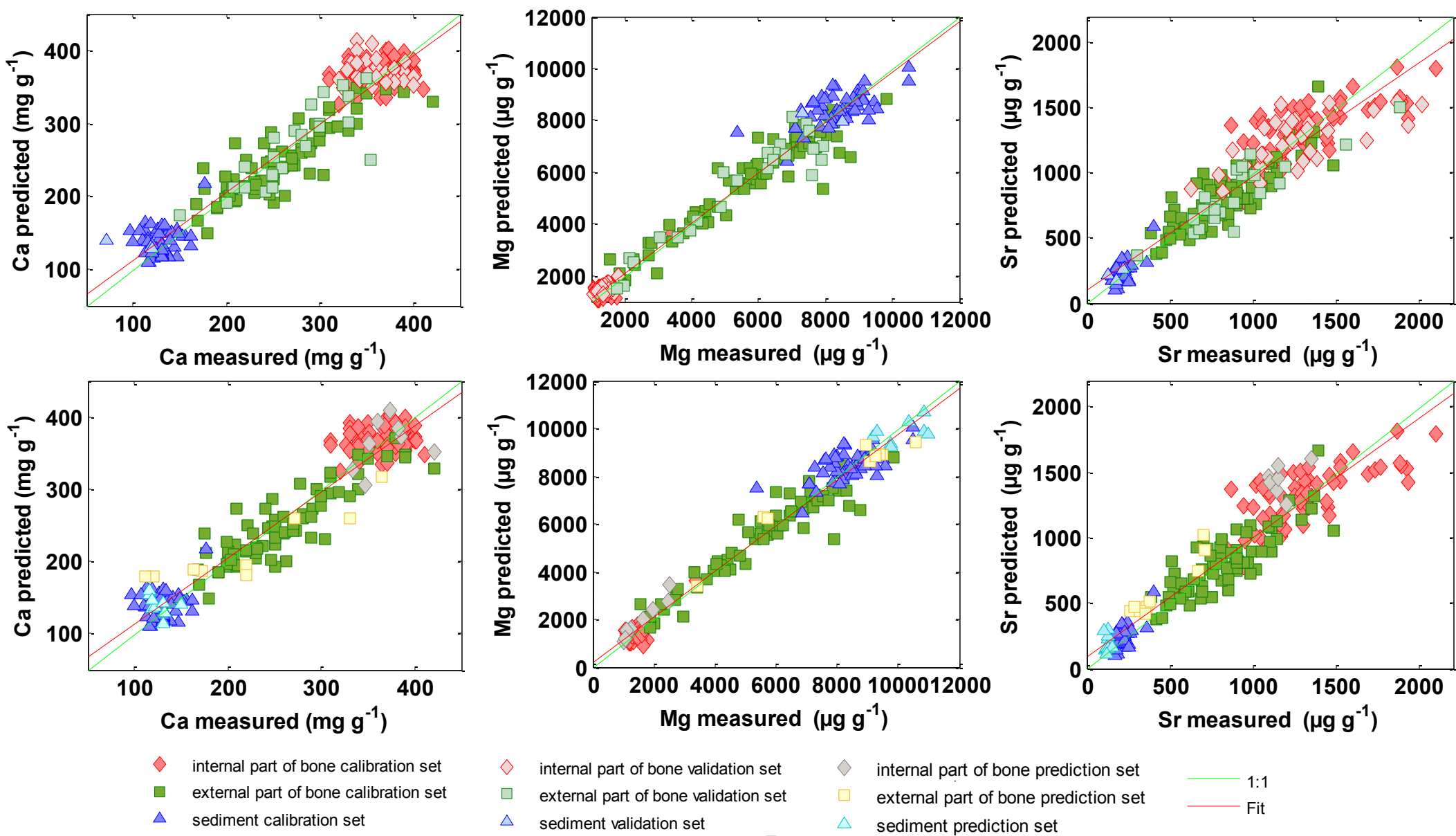


Figure 3. Regression between predicted and reference values obtained for the PLS-NIR determination of calcium, magnesium and strontium in bone remains and sediments